

Estimating uncertainty in the chronology of englacial radar stratigraphy chronology in Central West Antarctica

Gail, Charles, Duncan, Don

ABSTRACT.

The Byrd ice core, the first deep ice core drilled in Antarctica, is in a prime position to contribute to studies of the West Antarctic Ice Sheet's response to climate change. We use correlation between the Byrd ice core and laterally-extensive ice-penetrating radar to date englacial reflectors throughout the West Antarctic Ice Sheet. However, the Byrd ice core chronology is relatively poor due to limitations in drilling technology a lack of thorough uncertainty analysis. To address this, we construct a Bayesian estimate of age-depth profiles and uncertainty in the deep Byrd ice core chronology. Our result is validated against the recently-drilled WAIS Divide ice core chronology using isochronous englacial layers observed using ice-penetrating radar. We interpolate isochronous surfaces of four ages which sample the ice depth and observe that...

INTRODUCTION

The Byrd ice core (80.0167°S , 119.5167°W) was the first to be drilled to bedrock in Antarctica [Gow *et al.*, 1968]. The proximity of the core to fast-changing ice of both the Siple and Amundsen Sea coasts in West Antarctica make it a potentially important source of information in studies of the response of the West Antarctic Ice Sheet (WAIS) to changing climatic conditions. More than three extensive radar surveys passing near the core site, including the recent GIMBLE survey filling a data coverage gap in Marie Byrd Land [?], make it particularly useful for dating paleo ice dynamics observed in the central WAIS. Dated englacial radar data enables information from the entire ice volume—rather than only surface observations—to constrain ice dynamics in the central WAIS, including the Thwaites Glacier catchment and Marie Byrd Land.

While the Byrd ice core has been dated to more than 90ka [?], nearly back to the Last Interglacial, the chronology lacks estimates of uncertainty in age and depth. Here we use a Bayesian technique to compute a probabilistic chronology for the Byrd ice core which is constrained by existing ice core chronology results. This method inverts for probability distributions of ice sheet parameter values consistent with the recorded ice core chronology.

We use the modeled chronology to assign ages to englacial reflectors traced through the central WAIS. These reflectors encode information about ice sheet boundary conditions and paleo ice dynamics [e.g.]. They are the result of dielectric contrasts in the ice due to variations in composition, crystal fabric, temperature, and other ice properties. Each continuous reflector is assumed to be the result of a distinct surface deposition episode with a distinguishable dielectric signature and is therefore assumed to be isochronous [Fujita *et al.*, 2000].

The isochronous nature of englacial reflectors implies that assigning an age to each reflector at the Byrd ice core site effectively dates the reflector anywhere it can be continuously traced in the region. This allows for extensive age registration throughout the ice column and radar survey domain and also for validation of our results at the Byrd ice core with the recently-drilled WAIS Divide ice core chronology, as has been done in East Antarctica [Cavitt *et al.*, 2016]. The WAIS Divide ice core (79.48°S , 112.11°W) provides an ice chronology with uncertainty quantification as far as back as 67ka [Buizert *et al.*, 2015, C. Buizert, personal communication] and is therefore an independent validation of our improved Byrd ice core chronology.

Having two ice cores from which to date englacial reflectors enables more extensive dating, particularly in areas of complicated basal topography where the radar isochrones experience increased discontinuity and cannot be tracked for long distances. This is the case near the Marie Byrd Land icecap, for example, where reflectors present at the Byrd ice core site have been traced around areas of disruption due to high-relief bed terrain. In general, deeper reflectors are more difficult to track extensively in the WAIS due to lower reflection amplitudes and increased disruption. However, we interpolate three-dimensional isochronous surfaces for the extent of each of four observed reflectors which sample the ice depth. The modeled chronology is used to assign ages to these surfaces.

Section discusses the ice flow model used and the estimation of an age uncertainty envelope for the Byrd ice core. Section ?? introduces ice-penetrating radar data collected in the region and compares the age of selected reflectors determined at the Byrd and WAIS Divide ice cores.

POSTERIOR DISTRIBUTION OF ENGLACIAL REFLECTOR AGE-DEPTH

The Byrd ice core site lacks robust error analysis, so we derive uncertainty bounds for the Byrd ice core by computing the probability distribution of ice sheet parameters constrained by published ice core chronologies. Subsequent correlation to the WAIS Divide ice core is made using isochronous englacial reflectors which have been tracked between the two ice core sites.

We assume covariance in age as a function of depth and account for uncertainties in ice flow parameters such as accumulation rate over time to construct a self-consistent distribution of reflector ages.

To estimate the age-depth profile at the Byrd ice core, we use a Bayesian Markov Chain Monte Carlo technique to invert for the age and depth of observed englacial radar reflectors. This method preserves the depth correlation of the ice core chronology, estimates the probability of ice sheet parameter values, and develops a probabilistic estimate of the age-depth profile.

We derive an ensemble of age-depth profiles for the Byrd ice core constrained by agreement with a chronology of volcanic events from the past 50,000 years detected in the Byrd ice core record using the electrical conductivity method [Hammer *et al.*, 1997].

We assume a base level of 1% uncertainty on the volcanic ages and include a precision parameter, S , to quantify additional uncertainty. We invert for age given depth using a Bayesian Markov Chain Monte Carlo approach and check our result by correlation to the nearby WAIS Divide ice core chronology.

The Bayesian formulation of this problem is:

$$p(A_r) \sim p(D_r, \vec{f}, d_{firn}, v_{ice}, S | TWTT_r, A_{IC}, D_{IC}) \propto p(TWTT_r | D_r, d_{firn}, v_{ice}) p(A_{IC}, D_{IC} | \vec{f}, S) p(D_r, f, S) p(d_{firn}) p(v_{ice}) \quad (1)$$

Equation 1 describes how we will estimate the depths of four englacial reflectors (D_r), ice flow model parameters (\vec{f}), and a precision parameter on the uncertainty in the Byrd ice core chronology (S). Values for these quantities of interest will be informed by information about observed reflector two-way travel time to each reflector observed by from radar ($TWTT_r$) and the age-depth profile from the Byrd ice core volcanic record (A_{IC} , D_{IC}).

Priors on the quantities of interest as well as firn depth correction (d_{firn}) and velocity of electromagnetic waves in ice (v_{ice}), which contribute to errors in ice-penetrating radar depth, are used to put physical bounds on their values. Priors on D_r also preserve stratigraphic dependence of radar reflectors, requiring deeper reflectors be older than shallower reflectors. The first two factors on the right-hand side of Equation 1 are likelihood functions. These describe the probability that modeled results agree with observations: in the first, agreement between observed two-way travel time ($TWTT_r$) and modeled reflector depths (D_r) and in the second, agreement between flow model results (f) and the volcanic ages (A_{IC}).

The Metropolis algorithm is used to invert for parameter values consistent with observed ice core chronology and radar reflector data, effectively optimizing the likelihoods. Sets of parameter values for D_r , \vec{f} , S , d_{firn} , and v_{ice} are proposed which sample uncertainty in age and depth. Likelihood functions for age, $p(A_{IC} | D_{IC}, \vec{f}, S)$, and TWTT, $p(TWTT_r | D_r, d_{firn}, v_{ice})$, are evaluated to accept or reject proposed parameter sets based on how well they agree with the data. Accepted parameter values are those which are consistent with physical limits defined by the priors and with observations to within uncertainty. The resulting posterior probability distribution, $p(D_r, \vec{f}, S | TWTT_r, A_{IC}, D_{IC})$, can then be used to deterministically compute the corresponding probability distribution of the age of observed radar reflectors, $p(A_r)$, using the flow model described below.

Ice flow model at the Byrd ice core

Due to the inherent interdependence of stratigraphic age in the ice column, we use a flow model to simulate the age-depth relationship in the ice column. We use a simple, one-dimensional model of ice flow (Equation 2) which derives ice age from accumulation rate [Schwander *et al.*, 2001], assuming constant horizontal strain rate in the upper part of the ice sheet and a shear layer of thickness h at the bottom of the ice sheet, for which we invert. In the shear layer, the strain rate is assumed to decrease linearly and the bottom of the ice is assumed sliding with velocity $q \cdot v_0$, where v_0 is the horizontal velocity at the surface.

$$A(z) = \int_z^H \frac{dz}{\epsilon_z \dot{a}(z)} \quad (2)$$

where

$$\epsilon_z = \begin{cases} 1 - k(H - z), & h \leq z \leq H \\ kz(q + \frac{1-q}{2h}z), & 0 < z < h \end{cases}, \quad k = \frac{2}{2H-h(1-q)}$$

H is ice thickness in ice equivalent, z is height above the bed, h is the depth to the shear layer, \dot{a} is the layer thickness, and q is a constant for which we invert.

The ice flow model accounts for two primary factors in the age-depth profile: burial as a function of accumulation rate, \dot{a} , and thinning as a function of strain, ϵ_z . In the simplest realization, ice deposited at a given time at the ice sheet surface will be found at a depth in the ice sheet corresponding to the amount of subsequent accumulation. However, due to strain thinning at depth, the ice will be less deep than would be expected if accumulation alone is considered.

In Section , we invert for the flow parameters h , q , and \dot{a} . Constant values for h and q are sampled from uniform priors defined in a conservative range:

$$p(\vec{f}) = \begin{cases} p(h) \sim U(0, 0.5) \\ p(q) \sim U(0, 1) \\ p(\dot{a}_{z < 150m}) \sim U() \\ p(\dot{a}_{150 < z < 1024m}) \sim U() \\ p(\dot{a}_{1024 < z < 1200m}) \sim U() \\ p(\dot{a}_{1200 < z < 2164m}) \sim U() \\ \dots \text{update accums...} \end{cases}$$

The prior distributions of flow parameters, together denoted as $p(\vec{f})$, assume the shear layer is in the bottom half of the ice sheet depth and that the bed of the ice sheet is moving slower than the surface. Layer thickness, \dot{a} , is sampled from N distinct depth bins identified in observations by [Hammer *et al.*, 1997]. This allows for variability of layer thickness with depth, as expected. To limit unrealistic variability in accumulation between depth bins, Tikhonov regularization is used on the age likelihood function.

Radar depth and error

In addition to constraining the age of englacial reflectors by constructing an improved ice core chronology, we also quantify uncertainty in their radar-observed depth, another source of error in the age-depth profile. The ice-penetrating radar used in this analysis was collected in several surveys conducted by the University of Texas Institute for Geophysics, including GIMBLE [Young *et al.*, 2012], CASERTZ [?], and SOAR/WMB [Luyendyk *et al.*, 2003]. Data has been collected from a DC-3 or Twin Otter airborne platform and uses the HiCARS radar system with 60 MHz center frequency and 15 MHz bandwidth [Peters *et al.*, 2005].

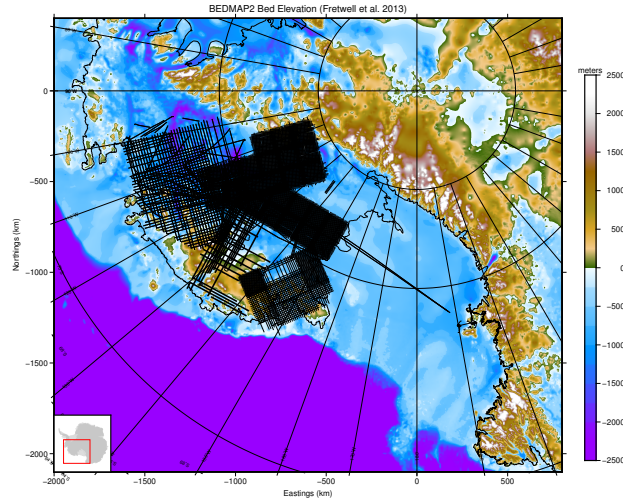


Fig. 1: Map of central West Antarctic with available airborne geophysical radar surveys (black lines) and (will be updated to have: WAIS Divide and Byrd ice core locations (blue triangles) overlain. Gray shading is surface elevation [Fretwell *et al.*, 2013].

HiCARS sends electromagnetic (EM) pulses into the ice from transmitting antennas mounted beneath the aircraft wings. Transmitted pulses reflect off surfaces of dielectric contrast in the ice which result from variations in ice fabric, composition, temperature, rheology, etc [Fujita *et al.*, 2000]. The reflected signal is received by the radar system and recorded as two-way travel time (TWTT) from transmission to receipt.

In this study, we consider TWTT of four reflectors from throughout the ice column in the region of central West Antarctica (Figure ??). These reflectors have been tracked extensively using Halliburton's Landmark seismic interpretation software and can be tied to the Byrd and/or WAIS Divide ice cores for dating purposes.

To estimate reflector depths, D_r , we begin with a simple relation assuming known velocity of the signal in air and in ice (first term in Equation 3). We also incorporate several known sources of uncertainty, including: 1) variations in the signal velocity in ice due to ice temperature and fabric, 2) vertical resolution limitations resulting from digitized pulse width sampling effects, and 3) measurement errors in the density profile needed to account for the changing signal velocity in firn (Equation 3).

$$D_i = \frac{1}{2} TWTT \cdot \vec{v} + \epsilon_{ice} + \epsilon_{PW} + \epsilon_{firn} \quad (3)$$

The first source of error, ϵ_v , results from ice temperature, crystal structure, anisotropy, and other ice fabric effects. EM velocity in ice, v_{ice} , varies from 168 to 169.5 m/ μ s [Fujita *et al.*, 2000] and the integration of these errors leads to increasing

depth uncertainty deeper in the ice. The complexity of local ice properties which may affect the velocity at any location and depth make it difficult to know the error distribution, so we make the simplifying and conservative assumption that this error is uniform. Constant values of v_{ice} are therefore sampled from a uniform distribution: $p(v_{ice}) \sim U(168 \text{ m}/\mu\text{s}, 169.5 \text{ m}/\mu\text{s})$.

The radar pulse width determines its vertical resolution [Millar, 1982]. We assume a finite pulse width, meaning that an infinitesimally thin layer of ice will appear in the survey to have a finite width. This can lead to errors in tracing reflectors and identifying their depths. The error in phase sampling of the EM pulse, ϵ_{PW} , is taken to be a function of the wavelength of the pulse, λ . The sampling rate for the data used here varies from 5 ns to 20 ns. We assume a 10 ns resolution when tracking the phase of layer detections and assume this error is normal.

Finally, in the upper part of the ice sheet, ice density profiles for the WAIS Divide [Kreutz et al., 2011] and Byrd [Gow et al., 1968] ice cores are used to correct for variations in radar signal velocity. All englacial reflectors of interest in this study are deeper than the firn layer, so a single firn correction is added to layer depths to accommodate the underestimation of depth if the firn layer is neglected. The firn correction, d_{firn} is treated as a model parameter for which we invert. Based on density measurements at the Byrd ice core site, bounds can be placed on the firn layer thickness and therefore the firn correction (the difference between the ice thickness with and without the firn layer present). We assume the firn correction to be less than the firn layer depth and sample values from a uniform distribution: $p(d_{firn}) \sim U()$.

We assume constant velocities, \vec{v} , in air (300 m/ μ s) and ice. The TWTT from the observing aircraft to the surface of the ice sheet is known from interpretation of the surface reflector and the remainder of the signal is assumed to be in ice. The computed depth of each reflector is relative to the ice surface as also measured by the HiCARS radar. While each layer may have depth errors independent of the others, errors in the distance between the surface and the acquisition aircraft are systematic across all observed reflectors in the ice column. Therefore, a randomly sampled error due to the vertical resolution is computed for the ice sheet surface and the same error is applied to all radar reflectors.

Metropolis Algorithm

At each iteration, the Metropolis algorithm proposes values for parameters of interest (those with priors in Equation 1). The algorithm accepts or rejects proposed sets of parameter values by comparison between the proposed and previously-accepted likelihood (or “cost”) values. A low cost value represents good agreement between model and observations, reflecting a small model-data misfit. Therefore, if the cost associated with proposed parameters is significantly lower than that of the last accepted iteration, the proposed parameter values have a high probability of being accepted as a more likely solution.

This process is repeated up to 50,000 times to create an ensemble of accepted parameter sets. These are used in the forward ice flow model to create an ensemble of age-depth profiles constrained by the combined uncertainty in the volcanic age-depth profile and ice model parameterizations. The resulting ensemble is expected to sample the age uncertainty in the Byrd ice core, providing the first robust uncertainty analysis of the ice core chronology.

There are two likelihood functions under consideration, describing the model-data misfit between reflector depth and age, respectively:

$$p(TWTT_r | D_r, d_{firn}, v_{ice}) = \exp\left[\frac{-\sum_{i=4}^4 [TWTT_{r,i} - TWTT_{m,i}(D_r)]^2}{2\sigma_{TWTT}^2}\right] \quad (4)$$

$$p(A_{IC} | D_{IC}, \vec{f}, S) = \exp\left[\frac{-S \sum_{j=53}^5 [A_{IC,j} - A_{m,j}(\vec{f}, D_{IC})]^2}{2\sigma_A^2}\right] + r \quad (5)$$

In the depth likelihood function, $TWTT_m(D_r)$ is based on the relationship between depth and TWTT as in Equation 3 and $TWTT_r$ is observed by ice-penetrating radar for each reflector. We assume depth errors could be correlated, but do not know the number of degrees of freedom a priori. To estimate the degrees of freedom, we invert the problem to calculate cost values from a perfect model to estimate degrees of freedom. Depth errors are assumed multivariate normal. The variance is proportional to the number of degrees of freedom such that

$$\frac{1}{\sigma_{TWTT}} = \frac{\sqrt{k_e/2}}{\sigma_{cost*}} \quad (6)$$

Here k_e is the number of degrees of freedom and $cost*$ represents the perfect model of TWTT which is perturbed with errors consistent with what we expect to find in the radar observations.

$$cost*_{TWTT} = \frac{\sum_{j=z}^z [TWTT_m(z) - \overline{TWTT_m}(z)]^2}{2} \quad (7)$$

In the age likelihood function, $j = 53$ represents the 53 volcanic events in the record used in this study. A_m comes from solutions to the forward ice flow model. A regularization term, r , is used to penalize large variability in the sampled accumulation function which is an input to the ice flow model. Due to poor knowledge of uncertainty in the volcanic record, we assume a baseline age uncertainty, σ_A , of 1%. A hierarchical Bayes approach then incorporates a precision parameter, S , which inverts for age uncertainty in our model as described in Jackson and Huerta [2016]:

$$S = Ga\left(\frac{k_e}{2} + \alpha, E_m + \beta\right) \quad (8)$$

Here shape and rate parameters, α and β , are assumed to be 1 as in the case for a noninformative gamma prior.

The number of degrees of freedom, k_e , is taken to be the number of elements on D_r ; this first-order assumption assumes independence between predicted horizons. E_m is simply the model-data misfit term from Equation 5.

$$E_m = \frac{\sum_j [A_{IC,j} - A_{m,j}(\vec{f}, D_{IC})]^2}{2\sigma_A^2} \quad (9)$$

The precision parameter is used to account for uncertainty in addition to the assumed 1% when finding an optimal age solution. New values of S are proposed for each Metropolis iteration, effectively optimizing for the radar age uncertainty in addition to the other parameters.

UPDATED BYRD ICE CORE CHRONOLOGY

Probability density functions generated by the metropolis algorithm sample uncertainty in the age and depth for each of four radar reflectors observed near the Byrd ice core. The results show the estimated age and depth converge to peaked gaussian distributions, with standard deviations generally increasing with depth and age as expected. The age of the observed reflectors increases dramatically with depth, with the oldest and deepest observed reflector dated to 35.43 ± 0.56 ka. These observed reflectors therefore span to before the Last Glacial Maximum.

Reflector	TWTT (μs)	Depth (m)			Age (a)		
		Mean	Median	σ	Mean	Median	σ
1	6.02	167.6	167.6	2.4	1200	1200	20
2	6.78	231.4	231.4	2.4	1770	1770	40
3	7.18	265.6	265.6	2.3	2100	2100	60
4	8.94	414.4	414.4	2.4	3510	3500	150

Table 1: **THESE VALUES NEED TO BE UPDATED TO THE LATEST.** Depth and age mean, median, and uncertainty for ten strong radar reflectors near Byrd Station, West Antarctica. The radar two-way travel time (TWTT) is given in column 1.

DISCUSSION

CONCLUSION

ACKNOWLEDGEMENTS

Robert, Shubhangi, Arami, Bekah, Varun, Benj, etc. Chad, Marie, etc.

References

- Buizert, C., et al., The wais divide deep ice core wd2014 chronology–part 1: Methane synchronization (68–31 ka bp) and the gas age–ice age difference, *Climate of the Past*, 11(2), 153–173, 2015.
- Cavitte, M. G., D. D. Blankenship, D. A. Young, D. M. Schroeder, F. Parrenin, E. Lemeur, J. A. Macgregor, and M. J. Siegert, Deep radiostratigraphy of the east antarctic plateau: connecting the dome c and vostok ice core sites, *Journal of Glaciology*, 62(232), 323–334, 2016.
- Fretwell, P., et al., Bedmap2: improved ice bed, surface and thickness datasets for antarctica, *The Cryosphere*, 7(1), 2013.
- Fujita, S., T. Matsuoka, T. Ishida, K. Matsuoka, and S. Mae, A summary of the complex dielectric permittivity of ice in the megahertz range and its applications for radar sounding of polar ice sheets, *Physics of Ice Core Records*, pp. 185–212, 2000.
- Gow, A. J., H. T. Ueda, and D. E. Garfield, Antarctic Ice Sheet: Preliminary Results of First Core Hole to Bedrock, *Science*, 161, 1011–1013, doi:10.1126/science.161.3845.1011, 1968.
- Hammer, C., H. Clausen, and C. Langway, 50,000 years of recorded global volcanism, *Climatic Change*, 35(1), 1–15, 1997.
- Jackson, C. S., and G. Huerta, Empirical bayes approach to climate model calibration, *Geoscientific Model Development Discussions*, 2016, 1–19, doi:10.5194/gmd-2016-20, 2016.
- Kreutz, K., B. Koffman, D. Breton, and G. Hamilton, Microparticle, conductivity, and density measurements from the wais divide deep ice core, antarctica, 2011.
- Luyendyk, B. P., D. S. Wilson, and C. S. Siddoway, Eastern margin of the Ross Sea Rift in western Marie Byrd Land, Antarctica: Crustal structure and tectonic development, *Geochemistry Geophysics Geosystems*, 4, doi:10.1029/2002GC000462., 2003.
- Millar, D., Acidity levels in ice sheets from radio echo-sounding, *Ann. Glaciol*, 3, 199–203, 1982.

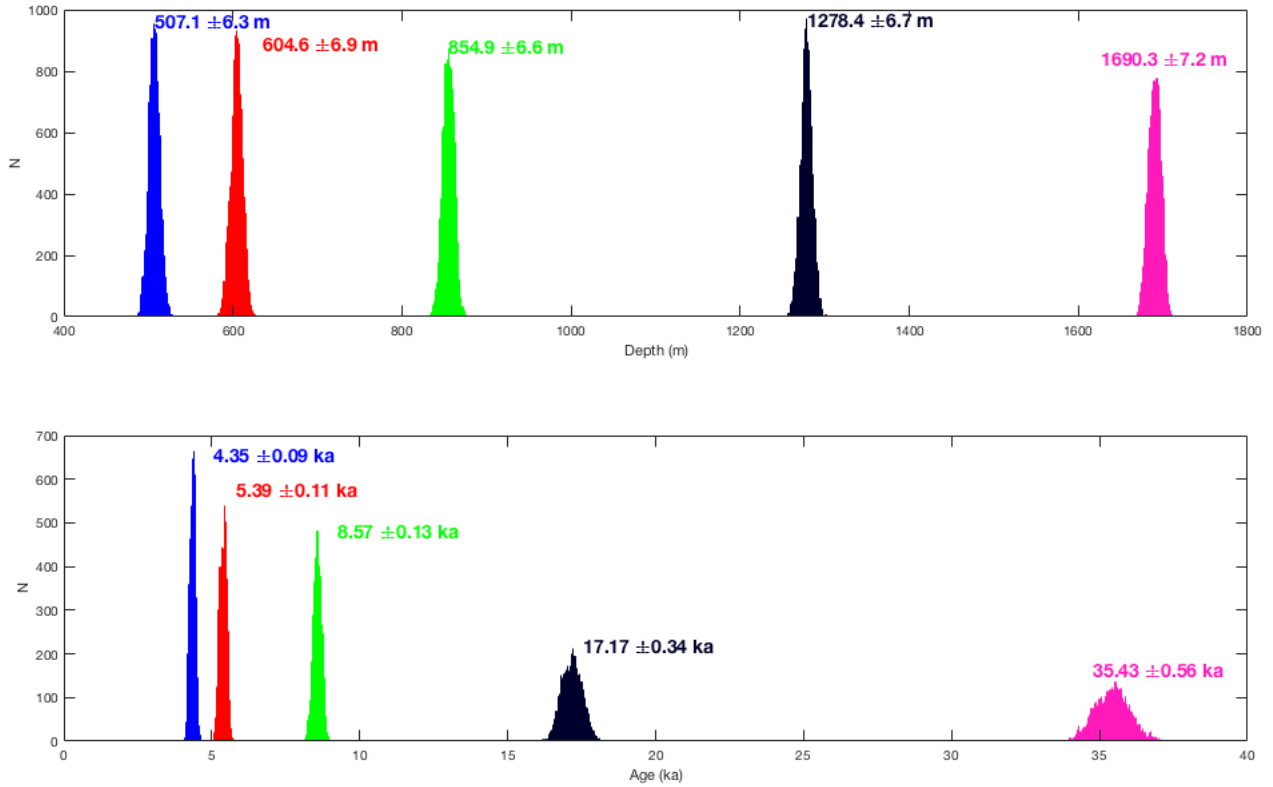


Fig. 2: Age and depth distributions of 5 layers which can be traced between WAIS Divide and Byrd ice cores. The width of the histograms represents uncertainty in estimates of layer age and depth, which increase with depth as expected.

- Peters, M. E., D. D. Blankenship, and D. L. Morse, Analysis techniques for coherent airborne radar sounding: Application to West Antarctic ice streams, *Journal of Geophysical Research (Solid Earth)*, 110, B06303, doi:10.1029/2004JB003222, 2005.
 Schwander, J., J. Jouzel, C. U. Hammer, J.-R. Petit, R. Udisti, and E. Wolff, A tentative chronology for the EPICA Dome Concordia ice core, *Geophysical Research Letters*, 28, 4243–4246, doi:10.1029/2000GL011981, 2001.
 Young, D. A., D. D. Blankenship, and J. W. Holt, GIMBLE: Geophysical Investigations of Marie Byrd Land Evolution: a new airborne survey of the linchpin of the West Antarctic, *WAIS Workshop 2012*, 2012.

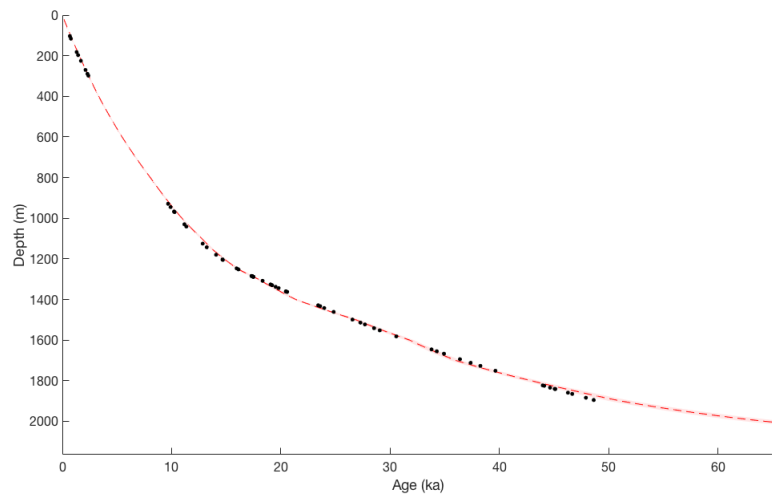


Fig. 3: Modeled age-depth relationship with uncertainty compared to measured volcanic chronology from ?.